

Stochastic model for nucleosome sliding under an external force

L. Mollazadeh-Beidokhti,¹ J. Deseigne,^{2,3} D. Lacoste,² F. Mohammad-Rafiee,¹ and H. Schiessel⁴

¹*Institute for Advanced Studies in Basic Sciences (IASBS), P.O. Box 45195-1159, Zanjan 45195, Iran*

²*Laboratoire de Physico-Chimie Théorique, UMR 7083, ESPCI, 10 rue Vauquelin, 75231 Paris Cedex 05, France*

³*Service de Physique de l'Etat Condensé, Centre d'Etudes de Saclay, CEA, 91191 Gif-sur-Yvette, France*

⁴*Instituut-Lorentz, Universiteit Leiden, Postbus 9506, 2300 RA Leiden, The Netherlands*

(Received 13 October 2008; published 30 March 2009)

Heat-induced diffusion of nucleosomes along DNA is an experimentally well-studied phenomenon, presumably induced by twist defects that propagate through the wrapped DNA portion. The diffusion constant depends dramatically on the local mechanical properties of the DNA and the presence of DNA-binding ligands. This has been quantitatively understood by a stochastic three-state model. Future experiments are expected to allow application of forces on the nucleosome that induce a directed sliding. By extending the three-state model, the present work studies theoretically the response of the nucleosome to such external forces and how it is affected by the mechanical properties of the DNA and the presence of DNA-binding ligands.

DOI: [10.1103/PhysRevE.79.031922](https://doi.org/10.1103/PhysRevE.79.031922)

PACS number(s): 87.15.A-, 87.15.H-, 87.15.Vv, 05.40.-a

I. INTRODUCTION

Eukaryotic DNA is packaged inside the nucleus by being wrapped onto millions of protein cylinders. Each cylinder is an octamer of eight histone proteins and is associated with a 147 base pair (bp) long stretch of DNA [1]. The resulting complexes, the nucleosomes, are connected via stretches of linker DNA; typical linker lengths range from 12 to 70 bp [2]. It is known from the crystal structure [1] that the DNA is bound to the octamer at 14 binding sites at which the minor groove of the DNA faces the octamer. This defines the binding path, a left-handed superhelix of one and three quarter turns.

With around three quarters of their DNA being tightly bound to the octamers, the DNA-binding proteins face the challenge that their target sites might be masked if they happen to be occupied by a nucleosome. One knows of two possible pathways of how such wrapped DNA portions become accessible—at least temporarily. One possibility is the spontaneous unwrapping of nucleosomal DNA from the octamer [3–5], which provides DNA-binding proteins a window of opportunity to bind to their target. Another possibility is that the octamer moves as a whole along the DNA [6–11], thereby releasing previously wrapped portions. This so-called nucleosome sliding is what we study in the following.

A typical experimental system for investigating nucleosome repositioning consists of a DNA template slightly longer than the wrapped portion (e.g., 207 bp in Ref. [7]) that is complexed with one octamer. The nucleosome position can be inferred from the electrophoretic mobility of the complex in a gel. It is found that nucleosome sliding is a slow process and that it takes a nucleosome around 1 h to reposition completely on such a short DNA fragment. Another important observation is that the new positions are all multiples of 10 bp (the DNA helical repeat) apart from the starting position.

Concerning nucleosome sliding there are currently two mechanisms under discussion that could underlie this phenomenon [9,10]. Both mechanisms have in common that they rely on defects that are thermally injected into the

wrapped DNA and that traverse the nucleosome, thereby causing its displacement. The reason for assuming defects as the cause of repositioning rather than the sliding of the octamer as a whole is that the latter mechanism would require the simultaneous detachment of all 14 binding sites that is too costly (around $85k_B T$). The two kinds of defects are 10-bp-loop defects [12,13] and 1-bp-twist defects [14,15]. A 10-bp-loop defect is a bulge that carries an extra length of 10 bp, causing redistribution events of that step length. These preserve the rotational orientation of the nucleosome. This fact as well as the predicted value for the mobility seems to agree with experiments [13].

The second class of defects, the 1-bp-twist defects, carries a missing or an extra base pair. To accommodate such a defect between two nucleosomal binding sites, the DNA needs to be stretched (or compressed) and twisted (hence the name). A nucleosome mobilized by twist defects moves via 1 bp jumps. Since the octamer is always bound to the minor groove of the DNA, the nucleosome performs a corkscrew motion around the DNA. Alternatively one can say that the DNA acts as a molecular corkscrew. Since twist defects are much cheaper than loop defects ($\approx 9k_B T$ [14] vs $\approx 23k_B T$ [13]), twist defects are expected to make nucleosomes much more mobile than observed in experiments. However, repositioning experiments are always done in the presence of so-called nucleosome positioning experiments that are now known to be widespread in eukaryotic genomes [16]. Such positioning sequences (such as the sea urchin's 5S ribosomal DNA (rDNA) sequence in Ref. [7]) make use of the fact that certain base-pair sequences induce an anisotropic bendability of the DNA. Since in the 1-bp-twist defect mechanism the DNA in the course of a 10 bp shift (the DNA's helical pitch) has to bend in all directions, a positioning sequence creates a sequence-specific barrier (not present for 10 bp bulges). In the case of the sea urchin's 5S rDNA sequence [7] this barrier is about $10k_B T$. It follows from equilibrium thermodynamics that the probability of finding the nucleosomal DNA in its preferred bending direction is much higher than in an unfavorable one. It means that even in the case of 1 bp defects, one would find nucleosomes mostly at the optimal positions 10 bp apart, i.e., at locations in the preferred bending

direction. In the end, both mechanisms are predicted to appear very similar in the above-mentioned experiments [10].

There is an experiment [17] that hints at twist defects being responsible for nucleosome sliding. This experiment is performed on a 216 bp DNA template that contains the sea urchin 5S rDNA sequence in the presence of minor-groove-binding pyrrole imidazole polyamides, synthetic ligands that can be designed to bind to short specific DNA sequences. It was found that the nucleosome mobility is dramatically reduced when such ligands are added.

In Ref. [15] a theoretical model was introduced to investigate the physics behind nucleosome sliding in the presence of ligands. The model gives a coarse-grained description of the nucleosome that is assumed to exist in three possible states that it encounters during its corkscrew diffusion along the DNA. The resulting diffusion constants for different possible cases give good agreement with experimental findings, supporting the picture of twist defects as the cause of nucleosomal mobility.

We anticipate that more experimental setups that can test nucleosomal mobility will become available in the near future. These setups will be all based on micromanipulation methods that allow application of forces to the nucleosome and study of its resulting sliding along the DNA. We mention three possible setups in Sec. V, at the end of this paper. It would be therefore helpful to have a model at hand that allows interpretation of data obtained by such experiments. In this context the three-state model proposed in Ref. [15] might prove to be of use but so far only the diffusion behavior in the absence of forces is known [15]. The purpose of the present paper is to close this gap by providing a general solution for a nucleosomal under force using the method described in Refs. [18,19].

The paper is organized as follows. In Sec. II the three-state model for nucleosomes is described and the behavior under an imposed force is calculated. Then we provide a section (Sec. III) on the diffusion of the nucleosome in the absence of an external force recovering relations found in Ref. [15]. This is followed by the largest section of this paper (Sec. IV), where we study the response of the nucleosome to an external force in the absence or presence of nucleosomal DNA positioning sequences and/or minor-groove-binding ligands. In the concluding section (Sec. V) we discuss possible experiments that could test our predictions.

II. STOCHASTIC THREE-STATE MODEL FOR NUCLEOSOME SLIDING

We reintroduce here the three-state model of Ref. [15] and then provide its general solution. In the absence of ligands, the sliding of the nucleosome along its wrapped DNA can be described by a hopping model with a single state or with two states depending on the DNA sequence. The effect of the sequence can be modeled as shown in Fig. 1 (without considering state 0 in this figure). State 1 represents the preferred binding sites for the DNA-histone complex (the minimum of the sequence-dependent potential), while state 2 corresponds to the high-energy state of this potential. For uniform sequences the height of the potential barrier is zero

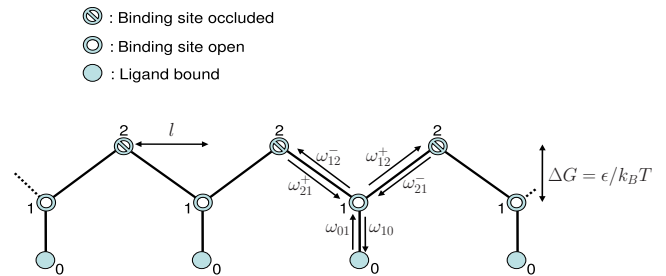


FIG. 1. (Color online) Schematic view of the three-state model for sliding of a nucleosome on a periodic DNA sequence of height $\Delta G = \epsilon k_B T$ and period $2l$. States 0, 1, and 2 denote states where the ligand is bound, unbound with its binding site open, and unbound with its binding site closed, respectively. $\omega_{ij}^{+(-)}$ denote the rates of going from state i to state j to the right (left).

(the energies of the two states are equal), which corresponds to a single-state model. For a positioning sequence of DNA, states 1 and 2 are separated by 5 bp, i.e., half of the period of the sequence denoted as l in the figure. Besides their widespread occurrence in eukaryotic DNA [16], such nucleosome positioning sequences can be artificially constructed. A very effective sequence arrangement, called the “TG” sequence, that leads to a strong nucleosome stability and localization was experimentally constructed in Ref. [20]. For this special sequence the system is in state 1 (2) when A/T (G/C) tracts are in the position of the nucleosome-binding sites.

Let us comment on why we do not use a ten-state model to describe the nucleosome motion along a positioning sequence with a 10 bp period. The problem in doing so would be that this introduces a large number of rate constants that are experimentally not accessible. Instead we prefer to follow here the coarse-grained approach introduced in Ref. [15] that amounts to considering only transitions between maxima and minima of the potential and neglects further microscopic details of the sequence. This coarse graining makes the model simpler without losing the underlying physics, especially allowing one to account for the strength of the positioning effect via the barrier height. Similar two-state models have been used to describe the motion of a linear molecular motor on its track (such as a kinesin walking on a microtubule) [18,19].

The presence of DNA ligands affects the interaction of the nucleosome with the DNA, and we describe this as an additional state 0 that branches off state 1 or 2. As described in Ref. [17] synthetic ligands, minor-groove-binding pyrrole imidazole polyamides, have been designed to bind to short specific DNA sequences (6 bp long). When the ligand binds to the DNA, we assume that no sliding can happen, as confirmed by experiments [17]. So the nucleosome waits until the ligand detaches from the DNA, and this will reduce the mobility of the nucleosome. The ligand may bind on the DNA in either state 1 and 2 depending on the location of its substrate, which is a short DNA sequence. In this model we only consider the case where the ligand can bind to the DNA when the nucleosome is in state 1. This is equivalent to $\Delta G > 0$ in Fig. 1. In state 2 (5 bp, half the DNA pitch, away from state 1) the binding site is then inaccessible since it faces the octamer surface. The case where a ligand can bind

to the nucleosome in state 2 has been shown—experimentally [17] and theoretically [15]—to leave the nucleosomal mobility nearly unaffected. Similar periodic sequential kinetic models with branching, jumping, or deaths have been studied in [21].

To model the dynamics of the nucleosome, consider the one-dimensional lattice of Fig. 1. The nucleosome can hop to neighboring sites on this lattice with some specific rates. Assume that l is the distance between sites 1 and 2 (which is half the period), and let $p_i(n, t)$ be the probability for the nucleosome to be in the states $i=0, 1, 2$ at position $x=nl$ and at time t . The $p_i(n, t)$ satisfy the master equation

$$\partial_t p_0(n, t) = \omega_{10} p_1(n, t) - \omega_{01} p_0(n, t), \quad (1)$$

$$\begin{aligned} \partial_t p_1(n, t) = & \omega_{21}^+ p_2(n-1, t) + \omega_{21}^- p_2(n+1, t) + \omega_{01} p_0(n, t) \\ & - (\omega_{12}^+ + \omega_{12}^- + \omega_{10}) p_1(n, t), \end{aligned} \quad (2)$$

$$\begin{aligned} \partial_t p_2(n, t) = & \omega_{12}^+ p_1(n-1, t) + \omega_{12}^- p_1(n+1, t) \\ & - (\omega_{21}^+ + \omega_{21}^-) p_2(n, t), \end{aligned} \quad (3)$$

where ω_{ij}^+ (ω_{ij}^-) represents the rate of transition from state i to neighboring state j on the right (left); and ω_{10} (ω_{01}) represents the binding (unbinding) rate of a ligand.

Let us introduce a vector $\vec{F}(\lambda, t)$, the components of which generate functions of the position for each state i . These components are $F_i(\lambda, t) = \sum_n e^{-\lambda n l} p_i(n, t)$. The use of generating function reduces the space of configurations that is infinite, to only three states, due to the periodicity of the system. It makes the calculations much more tractable. The master equation now becomes

$$\partial_t \vec{F}(\lambda, t) = M(\lambda) \vec{F}(\lambda, t), \quad (4)$$

with

$$M(\lambda) = \begin{bmatrix} -\omega_{01} & \omega_{10} & 0 \\ \omega_{01} & -\omega_{12}^+ - \omega_{12}^- - \omega_{10} & \omega_{21}^+ e^{-\lambda l} + \omega_{21}^- e^{\lambda l} \\ 0 & \omega_{12}^+ e^{-\lambda l} + \omega_{12}^- e^{\lambda l} & -\omega_{21}^+ - \omega_{21}^- \end{bmatrix}. \quad (5)$$

The solution of Eq. (4) is

$$\vec{F}(\lambda, t) = e^{M(\lambda)t} \vec{F}(\lambda, 0). \quad (6)$$

After calculating the eigenvalues of the matrix M , one can see that at long time $t \rightarrow +\infty$ only the largest eigenvalue of M that is denoted by $\sigma_m(\lambda)$ contributes to $\sum_i F_i(\lambda, t) = \langle e^{-\lambda n l} \rangle \sim e^{\sigma_m(\lambda)t}$. Note that the normalization condition for the probability implies that $\sigma_m(0)=0$. The eigenvalue $\sigma_m(\lambda)$ contains all the long-time dynamical properties of the system, such as the velocity and the diffusion constant [18,19], since

$$\bar{v} = - \left. \frac{d\sigma_m}{d\lambda} \right|_{\lambda=0} \quad (7)$$

and

$$D = \frac{1}{2} \left. \frac{d^2 \sigma_m}{d\lambda^2} \right|_{\lambda=0}. \quad (8)$$

One can expand $\sigma_m(\lambda)$ near $\lambda=0$ as $\sigma_m(\lambda) = -\bar{v}\lambda + D\lambda^2 + O(\lambda^3)$. Using this expansion in the eigenvalue equation, $\det[M - \sigma_m(\lambda)I_3] = 0$, the velocity and the diffusion constant are derived as

$$\bar{v} = \frac{2(\omega_{12}^+ \omega_{21}^+ - \omega_{12}^- \omega_{21}^-)l}{S + \frac{\omega_{10}}{\omega_{01}}(\omega_{21}^+ + \omega_{21}^-)}, \quad (9)$$

$$D = 2l^2 \frac{(\omega_{12}^+ \omega_{21}^+ + \omega_{12}^- \omega_{21}^-)K + 8\omega_{12}^+ \omega_{12}^- \omega_{21}^+ \omega_{21}^- + \frac{\omega_{10}}{\omega_{01}}J}{\left[S + \frac{\omega_{10}}{\omega_{01}}(\omega_{21}^+ + \omega_{21}^-) \right]^3}, \quad (10)$$

with

$$S = \omega_{12}^+ + \omega_{12}^- + \omega_{21}^+ + \omega_{21}^-, \quad (11)$$

$$K = (\omega_{12}^+)^2 + (\omega_{12}^-)^2 + (\omega_{21}^+)^2 + (\omega_{21}^-)^2 + 2(\omega_{12}^+ \omega_{12}^- + \omega_{12}^+ \omega_{21}^- + \omega_{21}^+ \omega_{21}^- + \omega_{21}^+ \omega_{12}^-), \quad (12)$$

$$J = (\omega_{12}^+ \omega_{21}^+ + \omega_{12}^- \omega_{21}^-)(\omega_{21}^+ + \omega_{21}^-) \left[2S + \frac{\omega_{10}}{\omega_{01}}(\omega_{21}^+ + \omega_{21}^-) \right] - 2(\omega_{12}^+ \omega_{21}^+ - \omega_{12}^- \omega_{21}^-)^2 \left[1 - \frac{\omega_{21}^+ + \omega_{21}^-}{\omega_{01}} \right]. \quad (13)$$

It is worth mentioning that in the ligand-free case the rate of going from site 1 to 0 is zero, $\omega_{10}=0$, and the model becomes equivalent to the two-state model that was discussed in [18,19].

III. KINETIC RATES IN THE ABSENCE OF FORCE

Nucleosome sliding in the absence of any external force is a passive process, implying that there is no preference between the left and right directions. Thus $\omega_{12}^+ = \omega_{12}^- = \omega_{12}$ and $\omega_{21}^+ = \omega_{21}^- = \omega_{21}$. Let us introduce κ as the ratio of rates,

$$\kappa \equiv \frac{\omega_{12}}{\omega_{21}} = e^{-\epsilon}, \quad (14)$$

where $\epsilon = \Delta G / k_B T$ is the energy difference between the two states 1 and 2, and the above equality expresses the detailed balance condition.

We consider the binding chemical reaction of the ligand: $L + S \rightleftharpoons LS$, where S is the substrate, i.e., the nucleosomal DNA, L is the ligand, and LS is the ligand-substrate complex. From kinetic theory of first-order chemical reactions, one can write $\omega_{10} = k_+ [L][S]$ and $\omega_{01} = k_- [LS]$, such that the equilibrium constant of the chemical reaction is $K_{eq} = k_+ / k_- = [LS]_{eq} / ([L]_{eq}[S]_{eq})$, in terms of equilibrium concentrations of ligand ($[L]_{eq}$), substrate ($[S]_{eq}$), and complex ($[LS]_{eq}$). Therefore the ratio

$$\eta \equiv \frac{\omega_{10}}{\omega_{01}} = K_{\text{eq}} \frac{[L][S]}{[LS]} = \frac{[LS]_{\text{eq}}}{[L]_{\text{eq}}[S]_{\text{eq}}} \frac{[L][S]}{[LS]} \quad (15)$$

quantifies the deviation away from equilibrium. In general, the substrate is in excess so that $[S]$ and $[S]_{\text{eq}}$ are both large, and also $[S] \approx [S]_{\text{eq}}$. Furthermore, if one assumes that $[LS] \approx [LS]_{\text{eq}}$, then $\eta \approx [L]/[L]_{\text{eq}}$.

From Eq. (9) we find that $\bar{v}=0$ as expected and from Eq. (10) we obtain the diffusion constant

$$D = \frac{2\omega_{12}l^2}{1 + \eta + \kappa}, \quad (16)$$

i.e., we recover Eq. (9) of Ref. [15].

The rate ω_{12} in Eq. (16) can be calculated by Kramers rate theory in the limit $\epsilon \gg 1$. We model the sequence-dependent potential as a periodic function $\beta U(x) = \frac{\epsilon}{2} \cos(\frac{\pi x}{l})$, with $\beta = 1/k_B T$ [14]. The time needed for the nucleosome to go from one minimum of this potential to the neighboring maximum, τ , is then given by

$$\frac{1}{\tau} = \frac{D_0}{2\pi k_B T} \sqrt{|U''(1)U''(2)|} e^{-\epsilon} = \frac{\pi|\epsilon|}{4l^2} D_0 e^{-\epsilon}, \quad (17)$$

where D_0 is the diffusion constant of the nucleosome without any potential barrier or ligand, and 1 and 2 refer to the minimum and the maximum of the potential $U(x)$. From this we find ω_{12} for such a strong positioning sequence:

$$\omega_{12} = \frac{1}{2\tau} = \frac{\pi\epsilon}{8l^2} D_0 e^{-\epsilon} \quad \text{for } \epsilon > 0, \quad (18)$$

with the factor $\frac{1}{2}$ being the probability to go through the barrier 2 from either direction [22]. It is worth mentioning that in the limit $\epsilon \gg 1$ with ($\epsilon > 0, \eta \geq 0$) when there is a sequence-dependent potential for the nucleosome, one can find that

$$D = \frac{\pi\epsilon e^{-\epsilon}}{4(1 + \eta)} D_0. \quad (19)$$

In the case of random sequence of DNA, i.e., in the absence of a sequence-dependent potential, $\epsilon=0$ and then ω_{12} is simply equal to

$$\omega_{12} = \frac{D_0}{l^2}, \quad (20)$$

and the diffusion constant can be found as [15]

$$D = \frac{2D_0}{2 + \eta}. \quad (21)$$

In the absence of ligands and for arbitrary sign of ϵ , Eq. (19) becomes

$$D = \frac{\pi|\epsilon|e^{-|\epsilon|}}{4} D_0. \quad (22)$$

Equation (22) that has been derived with a discrete stochastic model can be also derived using a continuous description in the limit $\epsilon \gg 1$. Consider a particle diffusing in the periodic potential $U(x)$. The resulting diffusion constant is then given by [22]

$$D = D_0 \langle e^{\beta U(x)} \rangle^{-1} \langle e^{-\beta U(x)} \rangle^{-1}. \quad (23)$$

Indeed $\langle e^{\beta U(x)} \rangle$ is a Bessel function, the asymptotic form of which is $2e^{\epsilon/2}/\sqrt{\pi\epsilon}$ for $\epsilon \gg 1$. From this Eq. (22) is recovered using Eq. (23).

Putting in numbers, using realistic parameter values [14] $D_0 \approx 600$ bp²/s, $\epsilon=9$, $l=5$ bp, and $\eta=0$ in the absence of ligands and $\eta \approx 100$ in the presence of ligands, our model predicts the time needed for a nucleosome to diffuse on a 70 bp DNA to be 78 min without ligands and 131 h with the ligands, which is consistent with the experimental observations [17]. For a random sequence ($\epsilon=0$), in the presence ($\eta \approx 100$) and the absence of ligands ($\eta \approx 0$), the characteristic times for 70 bp diffusion are 3.5 min and 4 s, respectively.

IV. FORCE-INDUCED NUCLEOSOME SLIDING

Up to now we considered thermally induced, undirected nucleosome sliding. Here we discuss the case when a force is applied to the nucleosome.

A force F exerted on the nucleosome introduces a bias in the transition rates:

$$\omega_{12}^+ = \omega e^{-\epsilon} e^{\theta_1^+ f}, \quad (24)$$

$$\omega_{21}^- = \omega e^{-\epsilon} e^{-\theta_2^- f}, \quad (25)$$

$$\omega_{12}^- = \omega e^{-\epsilon} e^{-\theta_1^- f}, \quad (26)$$

$$\omega_{21}^+ = \omega e^{\epsilon} e^{\theta_2^+ f}, \quad (27)$$

where θ_i^\pm are the load distribution factors [21], and $f \equiv Fl/k_B T$. Using detailed balance condition, one has $\theta_1^+ + \theta_1^- + \theta_2^+ + \theta_2^- = 2$. In the plots that follow we always use $\theta_i^\pm = 1/2$, but the possibility of other values is discussed at the end of this paper. Inserting these rates into Eq. (9), the velocity of the nucleosome is as follows:

$$v = 2\omega l e^{-\epsilon} \frac{e^{(\theta_1^+ + \theta_2^+)f} - e^{-(\theta_1^- + \theta_2^-)f}}{e^{-\epsilon}(e^{\theta_1^+ f} + e^{-\theta_1^- f}) + (1 + \eta)(e^{\theta_2^+ f} + e^{-\theta_2^- f})}. \quad (28)$$

The mobility of nucleosome is defined as

$$\mu \equiv \frac{1}{k_B T} \left. \frac{dv}{df} \right|_{f=0}, \quad (29)$$

which gives

$$\mu = \frac{1}{k_B T} \frac{2\omega\kappa}{1 + \eta + \kappa} l^2. \quad (30)$$

Comparing this expression with Eq. (16) one finds the Einstein relation $\mu = D/(k_B T)$ verified.

There are three physical quantities that affect the behavior of the system: the external force F , the sequence-dependent part of the potential measured by ϵ , and the ligand concentration $[L]$ that enters into η through $\eta \approx [L]/[L]_{\text{eq}}$. The physical behavior of the system is characterized by the velocity of the nucleosome repositioning along the DNA and its

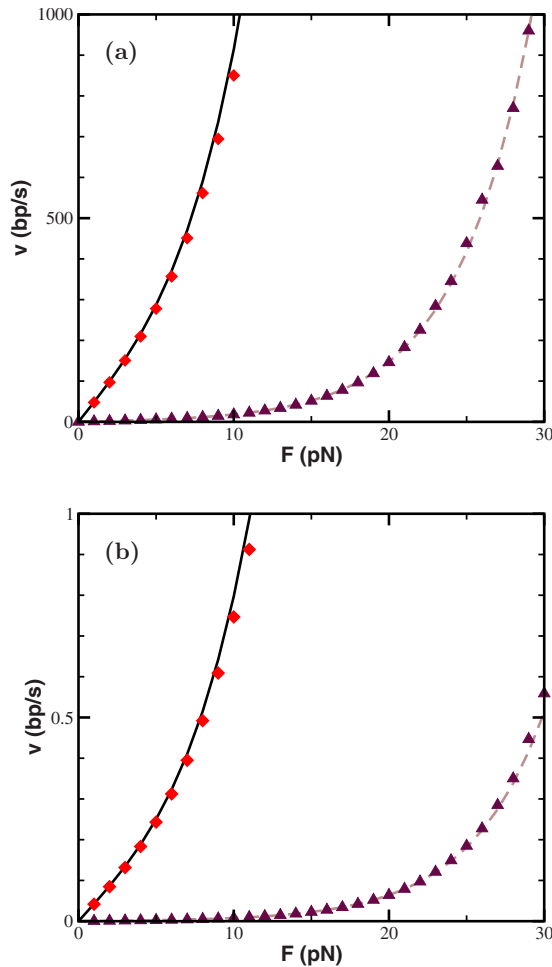


FIG. 2. (Color online) The velocity of the nucleosome versus the external force exerted on the nucleosome for (a) a random sequence of DNA ($\epsilon=0$) and (b) a positioning sequence with $\epsilon=9$ in two cases. The diamonds are simulation data for $\eta=0$, while the black solid line is plotted using theory [Eq. (28)]. The triangles are simulation data for $\eta=100$, while the brown dashed line is plotted using theory, again Eq. (28).

diffusive behavior. In the following the results of our analytical approach and of a computer simulation that is discussed in Appendix A, are presented.

We first consider the effect of an external force on the velocity of the nucleosome repositioning along the DNA. In Fig. 2 we plot the nucleosome velocity v versus the applied force F for the two limiting cases $\eta=0$ and $\eta=100$ of the experiments [17], both on random DNA and on a positioning sequence. In all four cases there is excellent agreement between the simulation results and the analytical approach. At zero force, the nucleosome shows purely diffusive behavior and there is no net velocity. As soon as a force is applied, there is a bias in the transition rates and the nucleosome attains a drift velocity in the direction of the applied force. A positioning sequence of DNA leads to an effective potential barrier on the corkscrew path of the nucleosome [14], leading to a drift that is significantly smaller than on random DNA. Finally, in the presence of ligands the corkscrew sliding is significantly hindered.

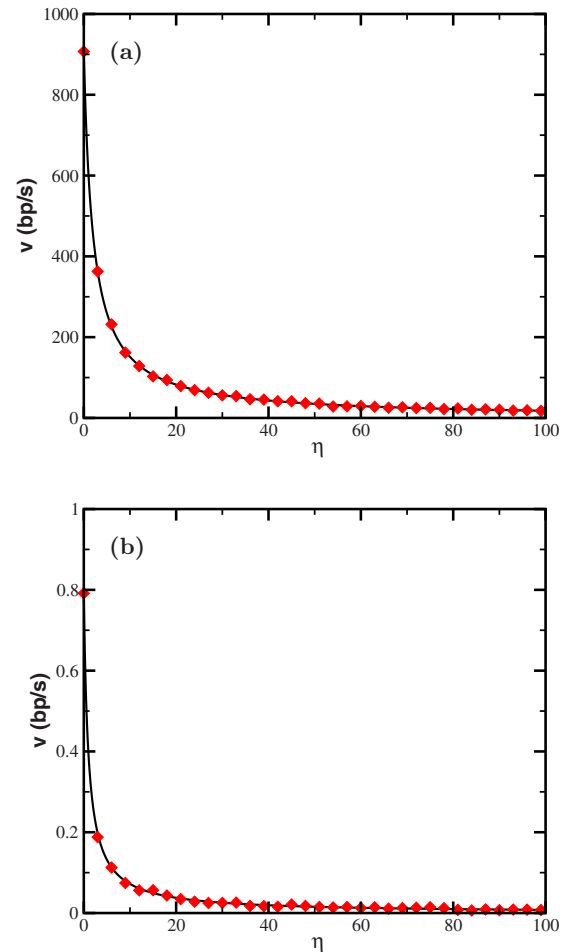


FIG. 3. (Color online) Velocity v of the nucleosome versus η in the presence of an external force $F=10$ pN on (a) a random base-pair sequence ($\epsilon=0$) and (b) a positioning element ($\epsilon=9$). The red diamonds are the simulation results, while the line is plotted using the analytical approach [Eq. (28)].

The influence of the ligand concentration on the sliding velocity for a typical external force of 10 pN is presented in Fig. 3. As can be seen from this plot, for typical experimental numbers [17] already a small concentration of ligands is sufficient to significantly lower the drift.

Another parameter that provides information about the system is the diffusion constant of the nucleosome, D . In Fig. 4 we present D as a function of the applied force F for the case of a positioning sequence. We find that D increases with the force in the ligand-free case as well as in the presence of ligands, $\eta=100$. That the diffusion constant increases with F is a typical effect and is, e.g., also found for ordinary biased diffusion on a lattice as discussed in Appendix B.

We present the behavior of the diffusion constant versus η , for two different forces, $F=0$ pN and $F=10$ pN, in Figs. 5 and 6. Naively one would expect that at a fixed external force the diffusion constant decreases with η since an increase in the ligand concentration leads to a higher probability to have a ligand bound that then suppresses diffusion. For zero force the diffusion constant does indeed follow this expectation; cf. Figs. 5(a) and 6(a). Interestingly, in the presence of a nonzero external force the behavior of the diffusion

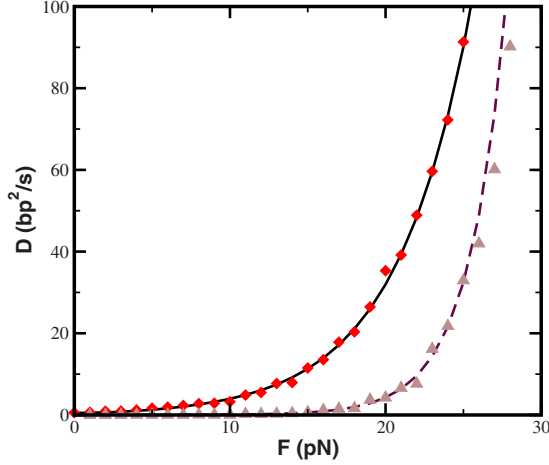


FIG. 4. (Color online) Diffusion constant D of the nucleosome versus external force F for a positioning sequence ($\epsilon=9$). The solid black line (red diamonds) and the brown dashed line (light brown triangles) are the theoretical (simulation) results for $\eta=0$ and $\eta=100$.

constant versus η differs dramatically from this expectation. For $\eta \lesssim 1$, D increases with η , and then decreases as η goes to infinity [Figs. 5(b) and 6(b)]. For random (positioning) DNA the maximal value of the diffusion constant is 5 (2) orders of magnitude larger than the value in the absence of ligands.

The η at which D attains its maximum η^* can be calculated from Eq. (10) and is shown in Fig. 7 as a function of F for the two cases of random and positioning DNAs. As can be seen in this figure η^* approaches quickly the values of 1 for random DNA and 0.5 for the positioning sequence. This can be read off the diffusion constant. Since at large forces the positive rates ω^+ dominate, Eq. (10) simplifies to

$$D = 2l^2 \frac{\eta(\omega_{12}^+ \omega_{21}^+)^2 \omega_{21}^+}{\omega_{01}[\omega_{21}^+(\eta+1) + \omega_{12}^+]^3}. \quad (31)$$

Setting the derivative of D with respect to η equal to zero, one obtains

$$\eta^* = \frac{\omega_{12}^+ + \omega_{21}^+}{2\omega_{21}^+} = \frac{1 + e^{-\epsilon + (\theta_1^+ - \theta_2^+)f}}{2}, \quad (32)$$

where we have used Eqs. (24)–(27). For the case $\theta_f^\pm = 1/2$ (the case depicted in Fig. 7) the force-dependent term drops out and we find $\eta^* = (1 + e^{-\epsilon})/2$. Thus one has indeed $\eta^* = 1$ for random DNA and $\eta^* = 1/2$ for a strong positioning sequence.

Let us now discuss the behavior of the diffusion constant versus η for small values of η , i.e., for $\eta \ll 1$. Through an expansion of the exact expression we obtain

$$D = A_0(f) + A_1(f)\eta + O(\eta^2), \quad (33)$$

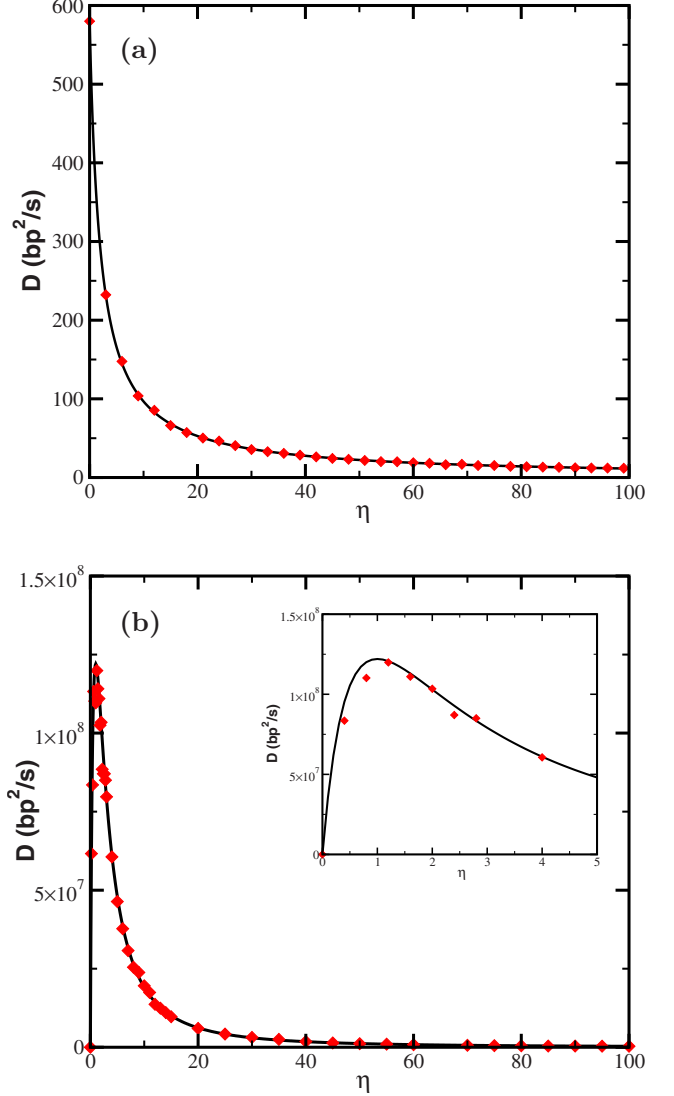


FIG. 5. (Color online) Nucleosome diffusion constant D versus η for random DNA ($\epsilon=0$) for two different forces: (a) $F=0$ pN and (b) $F=10$ pN. (The inset gives a zoomed view showing the non-monotonous behavior for small η values.) The red diamonds are the simulation results, while the lines are from using the analytical approach [Eq. (10)].

where A_0 and A_1 are functions of f that are given in Appendix C. It is convenient to expand $A_1(f)$ as a function of f :

$$A_1(f) = \left. \frac{\partial D}{\partial \eta} \right|_{\eta=0} = \alpha(\beta_0 + \beta_1 f^2) + O(f^4), \quad (34)$$

where α , β_0 , and β_1 are functions defined in Appendix C. Since $\alpha > 0$ and $\beta_0 < 0$, we have $\partial D / \partial \eta < 0$ for both random and positioning sequences of DNA at $f=0$ as can be verified by the plots in Figs. 5(a) and 6(a). When β_1 becomes positive, there is a threshold in force, $f_T = \sqrt{-\beta_0/\beta_1}$, such that for $f > f_T$ the derivative of D with respect to η is positive for small η values. From the explicit expressions for the coefficients given in Appendix C follows

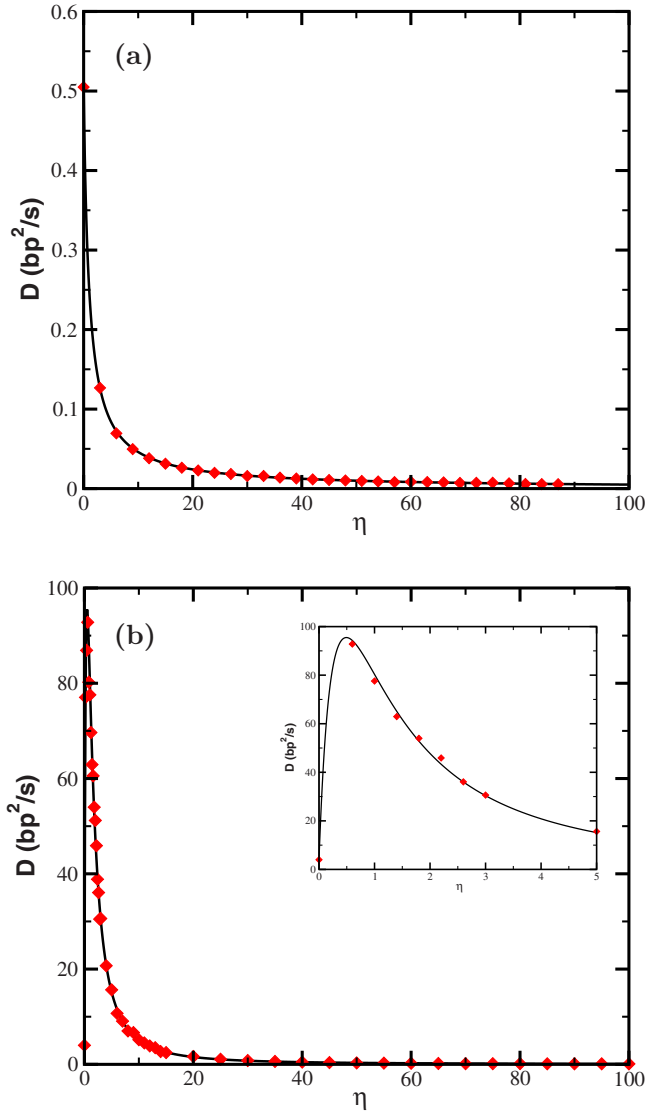


FIG. 6. (Color online) The diffusion constant of the nucleosome versus η in the case of a positioning sequence with $\epsilon=9$ for two different forces: (a) $F=0$ pN and (b) $F=10$ pN. The inset is the zoomed-in plot showing the behavior of the diffusion constant for small values of η . The red diamonds are the simulation results, while the lines are plotted using the analytical approach.

$$f_T = \frac{\sqrt{2}(1 + e^{-\epsilon})}{\left[-3 + e^{-\epsilon}(5 - 6e^{-\epsilon}) + 4e^{-\epsilon}(1 + e^{-\epsilon}) \frac{\omega}{\omega_{01}} \right]^{1/2}}. \quad (35)$$

Putting in numbers, $\omega_{01}=0.001 \text{ s}^{-1}$ and $\omega=D_0/l^2 \approx 24 \text{ s}^{-1}$, we find $f_T \approx 0.48$, which is equivalent to $F \approx 0.016$ pN for a random sequence of DNA. In the case of the positioning sequence the rate of ω changes to $\omega = \pi \epsilon D_0 / (8l^2) \approx 85 \text{ s}^{-1}$ and we find $f_T \approx 0.23$, which is equivalent to $F \approx 0.55$ pN. These threshold forces can indeed be read off the plots in Fig. 7 as the forces at which the corresponding η^* start to attain a positive value.

How can the surprising nonmonotonous dependence of D on η for a nucleosome under force be explained, especially

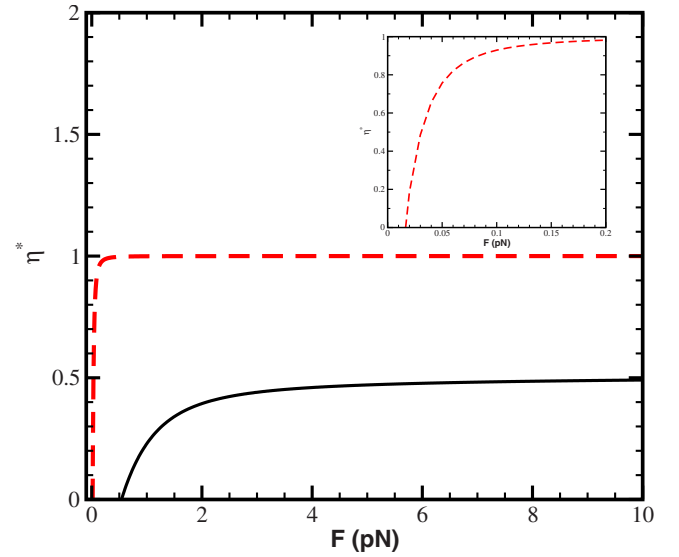


FIG. 7. (Color online) η^* versus F for the case $\theta_i^\pm = 1/2$ for random DNA (dashed line) and a nucleosome positioning element (solid line). The lines are drawn using Eq. (32).

the strongly enhanced fluctuations around η^* with $D(\eta^*) \gg D(\eta=0)$? Obviously the fluctuations in position for a driven nucleosome in the presence of ligands are of different origin from the ones in the absence of ligands. For sufficiently large forces the nucleosome mostly steps in the direction of the force or—if the nucleosome is in state 1—a ligand might bind. The latter event stops the drifting nucleosome for a while and is thus a source of fluctuations of completely different origin, effectively introducing a wide waiting time distribution for nucleosome escape from states 1 to neighboring states 2. The higher the concentration of ligands is, i.e., the higher the value of η is, the more often these events occur, increasing their contribution to the overall fluctuations in the nucleosome position, which are measured by the diffusion coefficient. This is the case up to a critical value of η , η^* . Further addition of ligands populates state 0 so much that the nucleosome is mostly stuck all the time, leading to a decrease in the value of D .

V. DISCUSSION

Within the framework of a stochastic three-state model, we have studied the mobility of a nucleosome along DNA in various cases. In the force-free case we recovered results from a previous publication [15] that showed that the diffusion constant is extremely sensitive to the underlying DNA mechanics and the presence of DNA-binding ligands: nucleosome positioning sequences and minor-groove-binding ligands reduce the mobility by several orders of magnitude. In the current study we extended this model to allow for externally applied forces and calculated resulting drift velocities and diffusion constants. The most striking feature that we found is a nonmonotonous dependence of the diffusion constant on the ligand concentration, for sufficiently large applied forces; cf. Figs. 5(b) and 6(b). The maximal value of the diffusion constant occurs at some intermediate

concentration η^* where the diffusion constant is typically several orders of magnitude larger than for the ligand-free case.

We note that the value of η^* depends according to Eq. (32) on the load distribution factors θ_i^\pm . Also other quantities depend on those factors. We assumed in all the plots that all θ_i^\pm are equal to $\frac{1}{2}$. By changing the values of θ_i^\pm the overall behavior of all plots does not change, although the precise values of the diffusion coefficient and even the curvature of the plots can be affected. The microscopic details of the interaction between the DNA and the nucleosome determine the values of the distribution factors. For a random sequence there is no reason to have different rates for backward and forward steps of the nucleosome along the DNA. Therefore, one finds that for large values of the external force, η^* converges to 1. For a DNA positioning sequence, the values of θ_i^\pm depend in principle on the precise energy landscape that results from the underlying sequence. The exact values of these coefficients can only be determined from experimental data or from a more detailed modeling of the transition state. We have arbitrarily chosen them to be 1/2 for the plots. Note that if $\theta_1^+ < \theta_2^+$ then $\eta^*|_{F \rightarrow \infty} = 0.5$, the same value as in our case $\theta_1^+ = \theta_2^+$, while for $\theta_1^+ > \theta_2^+$, η^* increases as F is increased and one has $\eta^*|_{F \rightarrow \infty} \rightarrow \infty$.

We finally discuss three possible experimental setups for applying forces on nucleosomes. The first setup could be achieved by holding a DNA with a positioned nucleosome under a small tension in a micromanipulation setup. One could then optically follow the interaction between a transcribing RNA polymerase and the nucleosome on its way if both complexes are fluorescently labeled. This experiment would be especially of interest since one should expect in eukaryotes frequent encounters between nucleosomes and transcribing RNA polymerases. Since the force-velocity characteristics of some polymerases are known, one could hope to be able to deduce the forces that the polymerase exerts on the nucleosome.

In this context there are several words of caution in place. First of all one has to ask the question as to whether the polymerase would not unravel the wrapped DNA from the nucleosome—destroying the complex altogether, a case considered recently by Chou [23]. For the typical forces and velocities encountered this might, however, not be a likely scenario. A second possible scenario has been deduced from experiments with short DNA fragments carrying single nucleosomes. In such a setup a transcribing RNA polymerase (e.g., bacteriophage polymerase from T7 [17] and SP6 [24]) can transcribe the whole fragment, even though it is partially occupied by a nucleosome. An interpretation of how the polymerase negotiates with the nucleosome is, however, tricky since there are at least two possible explanations. The simpler explanation is that the polymerase crosses the nucleosome in a loop [24,25]. However, the alternative explanation [15] is that the polymerase pushes the nucleosome in front of it, pushing it off the template; before the octamer falls off it rebinds at the other DNA terminus. Interestingly, in the presence of ligands the polymerase stalls [17], pointing toward the second mechanism. Note that the former mechanism would allow a polymerase to negotiate with an array of nucleosomes, while the second does not (“traffic

jam”). In fact, experiments [26] show that RNA polymerase can only transcribe through an array and leave it intact if a nuclear cell extract is present. Otherwise the nucleosomes are stripped off the DNA.

It is thus quite possible that the above proposed experiment would indeed find that the polymerase is able to push a single nucleosome over a large distance along the DNA. But even if this is the case, a recent more microscopic study of the interaction between an RNA polymerase and a nucleosome has demonstrated that the response of the nucleosome to the polymerase cannot be deduced from the force-velocity characteristics of the polymerase alone [27]. Instead, the microscopic details of the polymerase propulsion mechanism have a strong impact on its capacity to reposition nucleosomes.

It is therefore more desirable to apply directly a well-defined force to the nucleosome. Here are at least two possible strategies: using nanopores [28] and using a second DNA chain as a scanning probe [29]. If one pulls a DNA chain through a nanopore that is larger in diameter than that of the DNA double helix but smaller than the nucleosome, one could apply controlled forces on the nucleosome. In the second case, one has a setup with four optical traps and wraps one DNA chain tightly around the second, allowing to scan along the second chain. It has to be seen whether predictions done in the current work can be verified by some of those possible experiments.

ACKNOWLEDGMENTS

We are thankful to G. Wuite, C. Dekker, K. Mallick, and H. Fazli for valuable discussions. D.L. acknowledges support from the Indo-French center CEFIPRA (Grant No. 3504-2). F.M.-R. acknowledges financial support from ANR through Grant No. ANR JC0546258 and the hospitality of Laboratoire de Physico-Chimie Théorique, UMR 7083, ESPCI in Paris, where this work was initiated.

APPENDIX A: THE ALGORITHM OF THE SIMULATION

The three-state model presented in this paper is simulated using a “random selection method” [30]. It is defined in terms of the transition rates ω_{ij}^\pm that give the probabilities per unit time for going from state i to state j in the plus/minus direction. If the system is at time t in the state i , a transition to the neighboring state j happens at time $t + \Delta t$ with the finite probability $P_{ij}^\pm = \Delta t \omega_{ij}^\pm$.

For each step, a random number $0 \leq \xi < 1$ is drawn. Depending on its value and the state of the system, a decision is taken as follows:

$$\text{state: } 0 \rightarrow 1 \quad \text{if } 0 \leq \xi < P_{01},$$

$$\text{state: } 0 \rightarrow 0 \quad \text{otherwise,}$$

$$\text{state: } 1 \rightarrow 0 \quad \text{if } 0 \leq \xi < P_{10},$$

$$\text{state: } 1 \rightarrow 2^+ \quad \text{if } P_{10} \leq \xi < P_{10} + P_{12}^+,$$

state: $1 \rightarrow 2^-$ if $P_{10} + P_{12}^+ \leq \xi < P_{10} + P_{12}^+ + P_{12}^-$,

state: $1 \rightarrow 1$ otherwise,

state: $2 \rightarrow 1^+$ if $0 \leq \xi < P_{21}^+$,

state: $2 \rightarrow 1^-$ if $P_{21}^+ \leq \xi < P_{21}^+ + P_{21}^-$,

state: $2 \rightarrow 2$ otherwise.

For the next time step, from $t + \Delta t$ to $t + 2\Delta t$, the procedure is repeated again. The time step Δt is chosen small enough, such that for each step the condition $\sum \omega_{ij}^\pm \Delta t < 1$ is satisfied, where the sum is taken over the probabilities of all possible transitions from state i .

This algorithm is similar to the one of Gillespie [31], except for the fact that we use here a constant time step, whereas for the Gillespie algorithm the time step is a random variable. Both algorithms converge to the same steady state albeit after different times as we also checked for our model. The steady-state probabilities for the three states are obtained by setting the time derivatives of the probabilities in Eqs. (1)–(3) to zero,

$$p_0 = \frac{\eta}{1 + \eta + e^{-\epsilon}}, \quad (\text{A1})$$

$$p_1 = \frac{1}{1 + \eta + e^{-\epsilon}}, \quad (\text{A2})$$

$$p_2 = \frac{e^{-\epsilon}}{1 + \eta + e^{-\epsilon}}, \quad (\text{A3})$$

a result that was previously obtained in Ref. [15]. We let the simulation run for a long time (from t_0 to t_N , with $t_i = i\Delta t$ and $N \gg 1$) to be sure that the system has reached equilibrium. Then averaged over M ensembles with $M \gg 1$, the mean velocity and the diffusion constant are determined by

$$v = \frac{\sum_{r=1}^M [X_r(t_N) - X_r(t_1)]}{N\Delta t M}, \quad (\text{A4})$$

and D is determined as the slope of the plot of $\sum_{r=1}^M X_r^2 / M - (\sum_{r=1}^M X_r / M)^2$ versus $2\sum_{r=1}^M t_r / M$.

The time steps used for the simulation are less than 0.001, depending on the simulated case. The time goes to 10^5 s, and the number of ensembles is $M=2000$. The used parameters for the simulation are $\theta_i^\pm = 1/2$, with $i=1,2$, and ω is determined from Eqs. (18) and (20) for the positioning and random DNA sequences, respectively. Also using the experimental data, the typical time needed for a ligand to unbound from the DNA is some minutes and $\omega_{01} = 0.001 \text{ s}^{-1}$.

APPENDIX B: BIASED DIFFUSION

To understand better the effect of an external force on the diffusion constant, we consider here simple diffusion on a

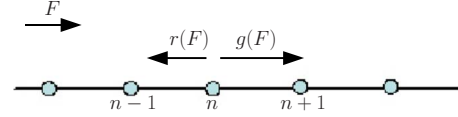


FIG. 8. (Color online) One-dimensional diffusion of a particle in the presence of an external force F . The force leads to an imbalance in the jumping rates $g(F)$ and $r(F)$ of the particle.

one-dimensional lattice; cf. Fig. 8, where the position of the particle is denoted by n . By definition, the diffusion constant is written as

$$D \equiv \frac{1}{2} \lim_{t \rightarrow \infty} \frac{\partial}{\partial t} [\langle n^2 \rangle - \langle n \rangle^2], \quad (\text{B1})$$

where $\langle A \rangle$ denotes the average of quantity A that is given by $\langle A \rangle = \sum_n A_n P_n$. P_n is the probability for the particle to be in the position n . The master equation governing this system can be written as

$$\frac{dP_n}{dt} = r(F)P_{n+1} + g(F)P_{n-1} - [r(F) + g(F)]P_n, \quad (\text{B2})$$

where the force is denoted by F , a is the jump length, and $g(F)$ and $r(F)$ are the force-dependent rates for going to the right and left, respectively. Here, we assume that the force pushes the system to the right so that $g(F)$ increases with F , while $r(F)$ decreases with F . Then a simple calculation leads to

$$\frac{\partial}{\partial t} \langle n^2 \rangle = 2[g(F) - r(F)]\langle n \rangle + g(F) + r(F), \quad (\text{B3})$$

$$\frac{\partial}{\partial t} \langle n \rangle^2 = 2[g(F) - r(F)]\langle n \rangle, \quad (\text{B4})$$

where we have used

$$\frac{\partial}{\partial t} \langle A \rangle = \sum_n A_n \frac{\partial}{\partial t} P_n, \quad (\text{B5})$$

$$\frac{\partial}{\partial t} \langle A \rangle^2 = 2\langle A \rangle \frac{\partial}{\partial t} \langle A_n \rangle, \quad (\text{B6})$$

and

$$\sum_n P_n = 1. \quad (\text{B7})$$

Using Eqs. (B3) and (B4) one finds for the diffusion constant

$$D = \frac{g(F) + r(F)}{2}. \quad (\text{B8})$$

If the rates in the absence of the external force are denoted by ω , the external force F changes the jumping rates of the particle to $g(F) = \omega \exp[+Fa/(2k_B T)]$ and $r(F) = \omega \exp[-Fa/(2k_B T)]$. Hence

$$D = \frac{\omega}{2}(e^{+Fa/2k_B T} + e^{-Fa/2k_B T}). \quad (\text{B9})$$

We find thus that the diffusion constant increases with F , similar to the observation in our three-state model; cf. Fig. 4.

APPENDIX C: THE EXPLICIT FORMS OF THE AUXILIARY FUNCTIONS

In this appendix we give the explicit form of the constants used in the Eqs. (33) and (34). First we expand D for $\eta \rightarrow 0$:

$$D = \frac{B_0 + B_1\eta + B_3\eta^2}{[S + B_2\eta]^3} = \frac{B_0}{S^3} + \frac{B_1S - 3B_0B_2}{S^4}\eta + O(\eta^2), \quad (\text{C1})$$

where

$$B_0 = 2l^2[K(\omega_{12}^+\omega_{21}^+ + \omega_{12}^-\omega_{21}^-) + 8\omega_{12}^+\omega_{21}^+\omega_{12}^-\omega_{21}^-],$$

$$B_1 = 2l^2 \left[2(\omega_{12}^+\omega_{21}^+ + \omega_{12}^-\omega_{21}^-)(\omega_{21}^+ + \omega_{21}^-)S - 2(\omega_{12}^+\omega_{21}^+ - \omega_{12}^-\omega_{21}^-)^2 \left(1 - \frac{\omega_{21}^- + \omega_{21}^+}{\omega_{01}} \right) \right],$$

$$B_2 = \omega_{21}^+ + \omega_{21}^-,$$

$$B_3 = 2l^2[(\omega_{21}^- + \omega_{21}^+)^2(\omega_{12}^+\omega_{21}^+ + \omega_{12}^-\omega_{21}^-)].$$

From this follow the expansion coefficients in Eq. (33):

$$A_0(f) = \frac{B_0}{S^3}, \quad (\text{C2})$$

$$A_1(f) = \frac{B_1S - 3B_0B_2}{S^4}. \quad (\text{C3})$$

Finally we provide here the behavior of $A_1(f)$ for small forces. Using Eqs. (24)–(27) with $\theta_i^\pm = 0.5$, the expansion of $B_i(f)$ for small forces can be written as

$$S = 2\omega(e^{-\epsilon} + 1) \left(1 + \frac{f^2}{4} \right),$$

$$B_0 = 8\omega^4 e^{-\epsilon}(e^{-\epsilon} + 1)^2 + 4\omega^4 e^{-\epsilon}[2 + 2e^{-2\epsilon} + (e^{-\epsilon} + 1)^2]f^2,$$

$$\frac{B_1}{2l^2} = 16\omega^4 e^{-\epsilon}(e^{-\epsilon} + 1) + \left[16\omega^4 e^{-2\epsilon} \left(1 + \frac{\omega}{\omega_{01}} + 24 \right) \right] f^2,$$

$$\frac{B_2}{2l^2} = 2\omega \left(1 + \frac{f^2}{4} \right).$$

Consequently,

$$A_1(f) = \frac{16l^2\omega^5}{S^4} e^{-\epsilon} \left\{ -2(1 + e^{-\epsilon})^2 + \left[-3 + e^{-\epsilon}(5 - 6e^{-\epsilon}) + 4e^{-\epsilon}(1 + e^{-\epsilon}) \frac{\omega}{\omega_{01}} \right] \right\}, \quad (\text{C4})$$

Using these expansions and Eq. (34), one can write

$$\alpha = \frac{16l^2\omega^5}{S^4} e^{-\epsilon}, \quad (\text{C5})$$

$$\beta_0 = -2(1 + e^{-\epsilon})^2, \quad (\text{C6})$$

$$\beta_1 = -3 + e^{-\epsilon}(5 - 6e^{-\epsilon}) + 4e^{-\epsilon}(1 + e^{-\epsilon}) \frac{\omega}{\omega_{01}}. \quad (\text{C7})$$

-
- [1] K. Luger, A. W. Mäder, R. K. Richmond, D. F. Sargent, and T. J. Richmond, *Nature (London)* **389**, 251 (1997).
[2] J. Widom, *Proc. Natl. Acad. Sci. U.S.A.* **89**, 1095 (1992).
[3] K. J. Polach and J. Widom, *J. Mol. Biol.* **254**, 130 (1995).
[4] G. Li, M. Levitus, C. Bustamante, and J. Widom, *Nat. Struct. Mol. Biol.* **12**, 46 (2005).
[5] W. Möbius, R. A. Neher, and U. Gerland, *Phys. Rev. Lett.* **97**, 208102 (2006).
[6] P. Beard, *Cell* **15**, 955 (1978).
[7] S. Pennings, G. Meersseman, and E. M. Bradbury, *J. Mol. Biol.* **220**, 101 (1991); G. Meersseman, S. Pennings, and E. M. Bradbury, *EMBO J.* **11**, 2951 (1992).
[8] A. Flaus and T. J. Richmond, *J. Mol. Biol.* **275**, 427 (1998).
[9] A. Flaus and T. Owen-Hughes, *Biopolymers* **68**, 563 (2003).
[10] H. Schiessel, *J. Phys.: Condens. Matter* **15**, R699 (2003).
[11] P. Ranjith, J. Yan, and J. F. Marko, *Proc. Natl. Acad. Sci. U.S.A.* **104**, 13649 (2007).
[12] H. Schiessel, J. Widom, R. F. Bruinsma, and W. M. Gelbart, *Phys. Rev. Lett.* **86**, 4414 (2001).
[13] I. M. Kulić and H. Schiessel, *Biophys. J.* **84**, 3197 (2003).
[14] I. M. Kulić and H. Schiessel, *Phys. Rev. Lett.* **91**, 148103 (2003).
[15] F. Mohammad-Rafiee, I. M. Kulić, and H. Schiessel, *J. Mol. Biol.* **344**, 47 (2004).
[16] E. Segal, Y. Fondufe-Mittendorf, L. Chen, A. Thåström, Y. Field, I. K. Moore, J.-P. Z. Wang, and J. Widom, *Nature (London)* **442**, 772 (2006).
[17] J. M. Gottesfeld, J. M. Belitsky, C. Melander, P. B. Dervan, and K. Luger, *J. Mol. Biol.* **321**, 249 (2002).
[18] A. W. C. Lau, D. Lacoste, and K. Mallick, *Phys. Rev. Lett.* **99**, 158102 (2007).
[19] D. Lacoste, A. W. C. Lau, and K. Mallick, *Phys. Rev. E* **78**, 011915 (2008).
[20] T. E. Shrader and D. M. Crothers, *Proc. Natl. Acad. Sci. U.S.A.* **86**, 7418 (1989); *J. Mol. Biol.* **216**, 69 (1990).
[21] A. B. Kolomeisky and M. E. Fisher, *Physica A* **279**, 1

- (2000).
- [22] P. Hänggi, P. Talkner, and M. Borkovec, *Rev. Mod. Phys.* **62**, 251 (1990).
- [23] T. Chou, *Phys. Rev. Lett.* **99**, 058105 (2007).
- [24] V. M. Studitsky, D. J. Clark, and G. Felsenfeld, *Cell* **76**, 371 (1994).
- [25] J. Bednar, V. M. Studitsky, S. A. Gregoryev, G. Felsenfeld, and C. L. Woodcock, *Mol. Cell* **4**, 377 (1999).
- [26] B. ten Heggeler-Bordier, C. Schild-Poulter, S. Chapel, and W. Wahli, *EMBO J.* **14**, 2561 (1995); B. ten Heggeler-Bordier, S. Muller, M. Monestier, and W. Wahli, *J. Mol. Biol.* **299**, 853 (2000).
- [27] L. Mollazadeh-Beidokhti, F. Mohammad-Rafiee, and H. Schiessel, *Biophys. J.* (to be published).
- [28] U. F. Keyser, B. N. Koeleman, S. van Dorp, D. Krapf, R. M. M. Smeets, S. G. Lemay, N. H. Dekker, and C. Dekker, *Nat. Phys.* **2**, 473 (2006).
- [29] M. C. Noom, B. van den Broek, J. van Mameren, and G. J. L. Wuite, *Nat. Methods* **4**, 1031 (2007).
- [30] T. H. Cormen, C. E. Leiserson, R. L. Rivest, and C. Stein, *Introduction to Algorithms*, 2nd ed. (MIT Press, Cambridge, MA/McGraw-Hill, New York, 1990).
- [31] D. T. Gillespie, *J. Phys. Chem.* **81**, 2340 (1977).